Supplemental data

Characterization of Bone Marrow Niche in patients with chronic myeloid leukemia Identifies CXCL14 as a New Therapeutic Option

Running title: Therapeutic potential of CXCL14 in CML

Monika Dolinska[1#], Huan Cai[1#], Alma Månsson[1#], Jingyi Shen[1], Pingnan Xiao[1], Thibault Bouderlique[1], Xidan Li[2], Elory Leonard[1], Marcus Chang[1], Yuchen Gao[1], Juan Pablo Medina Giménez[1], Makoto Kondo[1], Lakshmi Sandhow[1], Anne-Sofie Johansson[1], Stefan Deneberg[1], Stina Söderlund[3], Martin Jädersten[1], Johanna Ungerstedt[1], Magnus Tobiasson[1], Arne Östman[4], Satu Mustjoki[5,6,7], Leif Stenke[8], Katarina Le Blanc[9], Eva Hellström-Lindberg[1], Sören Lehmann[1,3], Marja Ekblom[10], Ulla Olsson-Strömberg[3], Mikael Sigvardsson[10,11] and Hong Qian[1*]

Content:

Additional Materials and Methods

Table S1 Characteristics of the patients with CML

Table S2 List of anti-human antibodies used for flow cytometry

Table S3 List of the antibodies used for intracellular marker staining

Table S4 List of probes used for Quantitative RT-PCR

Supplemental Figure 1-9

Supplemental references

* Correspondence to: hong.qian@ki.se

Additional Materials and Methods

CFU-F assay

CFU-F assay of freshly sorted BM MSCs or unfractionated MNCs was performed as previously described.[1] The cells were seeded at the density 100-200 cells/well for CD44$^-$ and 500-2000 cells/well for CD44$^+$ cells and cultured in hypoxic condition (1% O_2) for 14 days. The colonies were scored under an inverted microscope and clusters of more than 50 cells were counted as one CFU-F colony.

In vitro **multilineage differentiation assays**

This was done as described.[1] In brief, the osteoblast differentiation was induced in complete osteogenic medium mixed by Human/Mouse StemXVivo Osteogenic/Adipogenic Base Media (R&D Systems) and Human StemXVivo Osteogenic Supplement (R&D Systems) for 14-21 days. The cells were fixed with ice-cold methanol and stained with 1% Alizarin Red S (Sigma) (pH 4.1-4.3) for 10 min. The Alizarin Red staining was eluted with 10% (w/v) cetylpyridinium chloride (CPC) for 15min at room temperature and dye concentration was quantified by absorbance measurement at 562nm. For adipocyte differentiation, the cells were cultured in 20% oxygen in DMEM Glutamax (Gibco) supplemented with 10% FBS, 10 mM HEPES, 100 U/mL penicillin/streptomycin (HyClone), 10 μg/mL insulin (Sigma), 10^{-6} M dexamethasone (Sigma), 20 μM indomethacin (Sigma) or 0.5 mM isobutylmethylxanthine (Sigma). At day 14-21 after induction, the cells were fixed with 10% formalin and stained with 0.5% Oil Red O (Sigma) in isopropanol (Sigma). The Oil Red O staining was eluted with 100% isopropanol for 15 min at room temperature and dye concentration was quantified by absorbance measurement at 492 nm. The chondrocyte differentiation was induced in monolayer culture and in 3D pellets for 28 days. In both cases, the cells were cultured in 1% oxygen in complete DMEM + high glucose 4.5 g/L (Gibco) containing 10^{-7} M dexamethasone (Sigma), 1% ITS^{+3} (Sigma), 2 mM sodium pyruvate (Sigma), 0.35 mM proline (Sigma), 10 ng/ml TGF-β3 (R&D Systems) and 100 U/mL penicillin/streptomycin (HyClone). The chondrocyte differentiation after fixation with 10% formalin was verified by staining of proteoglycan with Toluidine blue (Sigma) (pH 2.0 to 2.5). For 3D pellet differentiation, 250 000 cells were placed in 15 mL Falcon tube, spun down 200xg, 5 min and the supernatant was discarded. The cells were then resuspended in 500 μL of complete chondrogenic media. At day 28 after induction, the 3D pellets were washed with PBS, fixed with PFA at 4°C, overnight and dehydrated in 20% sucrose. After fixation, pellets were transferred to cryomolds and frozen in TissueTeck® O.C.T™ Compound (Sakura)

in -80°C. Thereafter, the 3D pellets were cut with Cryostat (Leica CM3050) and 5 µm sections were stained with Toluidine blue (Sigma) (pH 2.0 to 2.5). The images were taken using fluorescence microscope Zeiss and Zen 2 software.

Fluorescence *in situ* hybridization (FISH) for *BCR* and *ABL1*

FACS-sorted CD45$^-$CD235A$^-$CD31$^-$CD44$^-$ MSCs, CD45$^-$CD235A$^-$CD31$^-$CD44$^+$ mature stromal cells, CD45$^-$CD235A$^-$CD31$^+$ ECs and CD45$^+$CD235A$^+$ hematopoietic cells were spun onto glass slides with low acceleration at 400 rpm for 5 min. The staining procedure was done, as described.[2] A background of 3-5% false positive was considered upon defining presence of BCR/ABL fusion gene in the cells.

FACS isolation of human hematopoietic stem and progenitor cells (HSPCs)

BM mononuclear cells were isolated by Ficoll-Hypaque (Lymphoprep, Axis-Shield PoC AS). The CD34$^+$ cells were enriched by magnetic activated cell sorting (MACS) using CD34 MicroBead Kit, human (Miltenyi Biotec). The purified CD34$^+$ or CD34$^+$CD38$^-$ BM cells were sorted by FACS AriaIII Cell Sorter (BD Biosciences) after staining with FC-blocker (mouse IgG, cat# 015-000-003, Jackson Immunoresearch) followed by monoclonal antibodies (BD Biosciences, unless otherwise specified), anti-CD34-APC (8G12) or BV421 (561) and anti-CD38-PECY7 or PE (HB7). The gate for CD34$^+$CD38$^-$ cells was set according to fluorescence-minus-one (FMO) controls and was 3-5% of the CD34$^+$ CML cells and normal NBM cells. The dead cells were excluded by propidium iodide (PI; Invitrogen) staining. See Table S2 for more information about anti-human antibodies used in the study.

FACS isolation and analysis of human BM MSCs

Mononuclear cells from BM aspirates from patients and healthy volunteers were isolated using Ficoll-Hypaque (Lymphoprep, Axis-Shield PoC AS) gradient density centrifugation as described[1]. The CD45$^-$GlycophorinA/CD235A$^-$ stromal cells were enriched by negative selection using CD45 and CD235A microbeads and magnetic-activated cell sorting (MACS) (Miltenyi Biotec). The enriched cells were first stained with mouse IgG (cat# 015-000-003, Jackson Immunoresearch) to block unspecific staining, subsequently with fluorochrome-conjugated anti-human antibodies CD45, CD235A, CD31, CD44, CD271, CD146, CD49D, CD140a, CD166, CD105, CD73, CD29, CD49F, CD106, CD90, CD184/CXCR4 for surface marker expression analysis and sorting. Dead cells were excluded by propidium iodine (PI

staining). Then CD45⁻CD235A⁻CD31⁻CD44⁻ MSCs, CD45⁻CD235A⁻CD31⁻CD44⁺ mature stromal cells and CD45⁻CD235A⁻CD31⁺ endothelial cells (ECs) were sorted. The cells were gated based on FMO controls and further analyzed and sorted on FACS Aria III (BD Biosciences). See Table S2 for more information about anti-human antibodies used in the study.

FACS analysis of intracellular molecule expression in MSCs

For analyzing intracellular marker expression in CML cells, BM MNCs or CD34 enriched cells from CML patients at diagnosis were first stained with mouse IgG whole molecule to block unspecific staining and subsequently with antibodies against CD34 and CD38, as described above. Then, the cells were fixed with 4% PFA for 10 min at room temperature, washed twice with 1x BD Perm/Wash™ buffer. After spinning down at 800 x g 5 min, the cells were stained with BD Phosflow™ Alexa Fluor® 647 mouse anti-mTOR (pS2448), cat#564242) or purified primary antibodies against OPA3 (ab230205), CYC1 (ab224044), SLC25A26 [EPR11581] (ab175209) and SERCA2 ATPase [EPR9392] (ab150435) in BD Perm/Wash™ buffer (BD 554723) overnight at 4°C. This was followed by staining with Alexa Fluor™ 647 donkey-anti-rabbit IgG secondary antibody (A31573, Invitrogen) for 60 min at room temperature.

For analyzing CXCL14 protein expression, FACS-sorted (CD45⁻CD235A⁻CD31⁻CD44⁻) and culture-expanded MSCs were first stained with recombinant anti-CXCL14 monoclonal antibody (EPR22807-28) (ab264467), and then by Alexa Fluor™ 647 donkey-anti-rabbit IgG secondary antibody (A31573, Invitrogen).

See more details about the antibodies for intracellular markers in Table S3.

RNA sequencing and data analysis

RNA from BM cell subsets sorted from CML patients and age-matched healthy donors were extracted using RNeasy microkit (Qiagen, USA) according to the manufacturer's recommendations. cDNA library was prepared by using the Ovation® Ultralow Library Systems (L2DR-BC1-16, NuGEN Technologies) and subjected to 76 cycles of NextSeq500 sequencing (Illumina) generating 20-30 million reads/sample. For CML CD34⁺CD38⁻ cells, cDNA was prepared using SMART-Seq v4 Ultra Low Input RNA Kit for Sequencing (Takara Bio). The cDNA quality was examined on Agilent TapeStation system using a High Sensitivity D5000 ScreenTape (Agilent). One ng cDNA was used for library preparation

using *Nextera XT* DNA Library Preparation Kit (FC-131-1024 & FC-131-1096, Illumina*). The yield and quality of the amplified libraries were analyzed using Qubit (Thermo Fisher Scientific) and the Agilent TapeStation System. The indexed cDNA libraries were normalized, combined and sequenced on the Illumina Nextseq 2000 for a 75-cycle v2 sequencing run generating 75 bp single-end reads.

All raw sequence reads available in FastQ format were mapped to the human genome (hg19) using Tophat2 combining with Bowtie2.[3,4] PCR duplicates were removed using samtools[5] after reads mapping. Next, raw reads mapped to each gene were calculated using FeatureCounts from Subread package.[6] Genes with Reads Per Kilobase of transcript per Million mapped reads (RPKM) values more than 0.1 were considered as being actively transcribed and proceeded to the analysis of Differential Gene Expression (DGE).[7] DEseq2 was used to perform the analysis of DGE, where genes with raw read counts were used as input. The differentially expressed genes were identified by adjust *P* value for multiple testing using Benjamini-Hochberg correction with False Discovery Rate (FDR) values less than 0.2.

For Gene Set Enrichment Analysis (GSEA), the read counts were first normalized by the Trimmed mean of M-values normalization method (TMM) [8] and then the normalized read counts were performed on the GSEA platform from Broad Institute (http://www.broadinstitute.org/gsea/index.jsp). The analyses were based on gene ontology (c5.all.v5.symbols.gmt), hallmark (h.all.v5.symbols.gmt) and KEGG (c2.kegg.v5.symbols.gmt). Gene sets with a nominal *P* value < .01 and FDR < .10 were considered to be significantly enriched. Those genes occurring in the ranked list before the point at which a maximal GSEA enrichment score is achieved are referred to as the leading-edge subset. Within each gene set, genes ranked in both the leftmost (indicates the strong positive correlation with the indicated phenotype) and rightmost (indicates the strong negative correlation with the phenotype), were referred to contribute to the leading edges effect for the core enrichment. The commonly altered genes among all BM cellular niche compartments were analysed by Venny 2.1 (http://bioinfogp.cnb.csic.es/tools/venny/index.html)[9].

RNA sequencing data are deposited at the National Center for Biotechnology Information (NCBI) with a GEO accession number GSE201122 for the CML CD34$^+$CD38$^-$ cells and GSE201398 for human BM stromal cells.

Colony-forming unit (CFU-C) assay of HSPCs

As described,[2,10] CD34$^+$CD38$^-$ or CD34$^+$ cells were cultured at a density of 50 or 150 cells/dish (for CD34$^+$ cells) or equivalent number of cells/dish (for CD34$^+$CD38$^-$ cells) in Methocult H4435 (Stem Cell Technologies) for their colony-forming capacity.

Co-culture of HSCs and LSCs with CXCL14-overexpressing fibroblasts

The control (NIH3-CTRL) and CXCL14-overexpressing NIH3T3 fibroblasts (NIH3-CXCL14) were established as described [11] and propagated in DMEM (Gibco) supplemented with 10% FBS (Gibco), 1% Glutamine (Gibco) and 1% penicillin/streptomycin (HyClone). For co-culture experiment, NIH3-CTRL or NIH3-CXCL14 cells were plated in 24-well plates at the density 30 000 cells/well in StemSpan™ Serum-Free Expansion Medium (SFEM) (Stem Cell Technology). After 24 hours, CD34$^+$CD38$^-$ cells from CML patients (LSCs) and healthy donors (HSCs) were FACS sorted and co-cultured with the NIH3-CTRL or NIH3-CXCL14 cells at density 200-1000 cells/well. After 7 days of co-culture, the cells were stained with fluorochrome-conjugated anti-human CD34, CD38, CD15, CD33, CD66b antibodies and analyzed by FACS. In addition, an aliquot of the cells were subjected to a long-term culture-initiating cells (LTC-IC) and colony-forming assay (CFU-C), as described [2]. Briefly, for LTC-IC assay, HSCs and LSCs after 7 days co-culture were plated into 200 μL Myelocult H5100 (Stem Cell Technologies), 10^{-6} M hydrocortisone (Sigma-Aldrich), 1% penicillin/streptomycin (HyClone) in plain 96-well microplates (BD Biosciences) on irradiated (8000 cGy) murine stromal cell lines Sl/Sl and M2-10B4 (5000 cells/cell type/well, mixed in 1:1 ratio). The cultures were maintained in normoxic conditions, at 37°C and 5% CO$_2$ for 6 weeks with weekly half-medium change and subsequently subjected to CFU-C assay. In some of the experiments, the cells at 3-4 days post the co-culture were transplanted into sublethally (250cGy) irradiated NSG-SGM3 mice at a dose of 1000 CD34$^+$CD38$^-$ cell equivalent/mouse for assessing CML LSC engraftment. The mice receiving the same donor were sacrificed simultaneously at 8- or 12-weeks post-transplantation when some mice started showing symptoms.

Quantitative RT-PCR

This was done as previously described.[12,13] See Table S4 for the information about Assays-on-Demand probes.

Measurement of mitochondria function by FACS

The effect of CXCL14 on mitochondrial function of CML cells was analyzed by FACS using a FACS-based protocol adapted from recently described[14]. Briefly, the cells were stimulated with either CXCL14 (10 ng/mL) or PBS at 500K cells/well in StemSpan SFEM (cat# 09650, StemCell Technologies) in 6-well tissue culture plate for 24h. K562 cells from CXCL14 stimulation and PBS were harvested and stained with 5 µM cell CellTrace violet (CTV, ThermoFisher Scientific, C34557) or PBS respectively, for 30 min at 37°C, followed by washing with PBS/10%FBS, the CTV-stained (CXCL14 stimulated K562 cells) and unstained cells (PBS stimulated K562 cells) were mixed and stained with 10 nM tetramethylrhodamine, methyl ester (TMRM) (Immunochemistry Technologies, 9105) for 40 min at 37 °C. The cells were then resuspended with 600 µL of MAS buffer containing 200 mM Mannitol (Sigma, 21673), 70 mM Sucrose (Sigma, S9378), 10 mM KH_2PO_4 (Sigma,), 5 mM MgCl2 (Sigma, M8266), 2 mM HEPES (Sigma, 15630056) and 1 mM EGTA (Sigma, E6758). To penetrate cell plasma membrane, the cell suspension was incubated with 30 µg/mL saponin (Sigma, S7900) at 37 °C for 10 min, and then stained with 10 nM TMRM. The basal mitochondria membrane potential (MMP) was recorded for 60s at PE channel, followed by 60s recording with dH_2O. To evaluate the mitochondrial complex I (NADH dehydrogenase) function on electron transporting chain (ETC), pyruvate (Sigma, 107360) and malate (Sigma, M0875) were added to cell suspension at 125 µM and 62.5 µM respectively, and incubated for 1 min, subsequently, subjected to 60s recording of MMP at PE-channel after 1 min incubation. After 60s recording with dH_2O, carbonyl cyanide-4 (trifluoromethoxy) phenylhydrazone (FCCP) (Abcam, ab120081) was added to the cell suspension at 1 µM, incubated for 1 min and recorded at PE channel for 60s. The data were analyzed for MMP kinetics in the cells by FlowJo 10.

Table S1 Characteristics of the newly diagnosed patients included in the study.

Patient ID	Age (y)	Gender	BCR-ABL transcript type	Other Cytogenetic abnormalities	spleen size, below costal margin (cm)
CML03	49	male	p210	no	25
CML05	68	male	p210	no	2
CML11	65	male	p210	no	0
CML13	68	female	p210	no	2
CML15	59	female	p210	no	18
CML16	69	female	p210	no	0
CML17	30	male	p210	no	6
CML18	28	female	p210	no	1
CML19	33	male	p210	no	3
CML20	57	female	p210	t(1;9;22)	0
CML21	69	female	p210	no	0
CML22	73	female	p210	no	0
CML24	30	male	p210	no	3
CML25	74	male	p210	no	0
CML27	23	female	p210	no	0
CML28	68	female	p210	no	0
CML30	60	female	p210	no	13
CML32	73	male	p210	no	3
CML33	37	male	p210	atypical fusion	12
CML34	78	female	p210	no	0
CML37	69	male	p210	no	Not known
CML39	45	female	p210	no	12
CML40	77	male	p210	no	0
CML44	55	male	p210	+8	12
CML48	62	male	p210		
CML50	21	male	p210	no	8
CML55	34	male	p210	no	0
CML56	37	male	p210	no	10
CML59	70	male	p210	no	0
CML61	51	male	p210		
CML62	85	female	p210	no	0
CML64	72	female	p210		
CML66	34	male	p210	no	2

Note: The patients marked in yellow are patients who failed to reach below 1% in BCR-ABL1 expression in BM or blood 6 months after TKI treatment start.

Table S2. List of anti-human antibodies used for flow cytometry.

Antibody		Conjugate	Clone	Catalog number	Company
Anti-human	CD235A	eFluor 450	6A7M	48-9884-42	eBioscience
Anti-human	CD45	eFluor 450	HI30	48-0459-42	eBioscience
Anti-human	CD45	Brilliant Violet 421	HI30	304029	BioLegend
Anti-human	CD34	Brilliant Violet 421	561	343610	BioLegend
Anti-human	CD31	PE-Cy7	WN59	303118	Biolegend
Anti-mouse/human	CD44	APC-Cy7	IM7	103028	BioLegend
Anti-human	CD271	FITC	ME20.4	345104	BioLegend
Anti-human	CD146	PE	SHM-57	342004	BioLegend
Anti-human	CD49D	PE	9F10	555503	BD Pharmingen
Anti-human	CD166	PE	3A6	343903	BioLegend
Anti-human	CD140a	PE	16A1	323505	BioLegend
Anti-human	CD73	APC	AD2	344005	BioLegend
Anti-human	CD29	APC	TS2/16	303007	BioLegend
Anti-mouse/human	CD49F	APC	GoH3	313615	BioLegend
Anti-human	CD45	APC	HI30	555485	BD Pharmingen
Anti-human	CD33	APC	WM-53	17-0338-42	eBioscience
Anti-human	CD105	Alexa Fluor 647	43A3	323212	BioLegend
Anti-human	CD106	PE-Cy5	STA	305808	BioLegend
Anti-human	CD90	PE-Cy5	5E10	328111	BioLegend
Anti-human	CD184/ CXCR4	PE-Cy5	12G5	306507	BioLegend
Anti-human	CD34	APC	8G12	348509	BD Bioscience
Anti-human	CD38	PE-Cy7	HB7	3358	BD Bioscience
Anti-human	CD15	FITC	HI98	555401	BD Pharmingen
Anti-human	CD33	FITC	HIM-3	555626	BD Pharmingen
Anti-human	CD66b	FITC	G10F5	561927	BD Pharmingen
Anti-human	CD3	APC-Cy7	SK7	557832	BD Pharmingen
Anti-human	CD19	PE	HIB19	302207	BD Bioscience
Anti-human	CD14	PE	HCD14	325605	BioLegend
Anti-human	CD45	Microbeads		130-045-801	Miltenyi Biotec
Anti-human	CD235A	Microbeads		130-050-501	Miltenyi Biotec

Table S3. List of antibodies used for intracellular marker staining.

Primary antibody	Dilution	Catalog number	Company
BD Phosflow™ Alexa Fluor® 647 Mouse Anti-mTOR (pS2448),	1/25	564242	BD Bioscience
Anti-OPA3 antibody	1:2000	ab230205	Abcam
Anti-CYC1 antibody	0.5 ug/ml	ab224044	Abcam
Anti-SLC25A26 antibody [EPR11581]	1:100	ab175209	Abcam
Anti-SERCA2 ATPase antibody [EPR9392]	1:800	ab150435	Abcam
Anti-SERCA2 ATPase antibody [EPR9392]	1:800	ab150435	Abcam
Recombinant anti-CXCL14 monoclonal antibody (EPR22807-28)	1:500	ab264467	Abcam

Table S4. List of probes used for Quantitative RT-PCR.

Gene name	Assay ID	Full name
ANGPT1	Hs00375822_m1	Angiopoietin 1
ANTPTL4	Hs01101127_m1	Angiopoietin like 4
BCR-ABL	Hs03043652_ft	BCR_ABL1 fusion
COL1A1	Hs00164004_m1	Collagen type I alpha I
COL2A1	Hs01060345_m1	Collagen type II alpha I chain
CXCL12	Hs03676656_mH	C-X-C motif chemokine ligand 12
CXCL14	Hs01557413_m1	C-X-C motif chemokine ligand 14
GAPDH	Hs02758991_g1	Glyceraldehyde-3-phosphate dehydrogenase
HPRT	Hs99999909_m1	Hypoxanthine guanine phosphoribosyl transferase
IL6	Hs00985639_m1	Interleukin 6
KITL	Hs00241497_m1	KIT ligand
LAMA4	Hs00935293_m1	Laminin subunit alpha 4

Supplementary Figure legends

Figure S1. The frequencies and differentiation capacity of BM stromal cells within total MNCs in healthy controls and CML patients.

(A) CFU-Fs are enriched in the CD44$^-$ stromal cells in aged-matched healthy (NBM) and CML BM. The colony numbers were normalized per 200 sorted CD44$^-$/CD44$^+$ stromal cells. (B) The frequencies of CD45$^-$CD235$^-$ total stromal cells within total BM mononuclear cells (MNCs). (C) The frequency of CD31$^+$ ECs, CD45$^-$CD235A$^-$CD31$^-$CD44$^-$ and CD146^{+-}CD271$^+$ MSC subsets and mature stromal cells (CD45$^-$CD235A$^-$CD31$^-$CD44$^+$) within total stromal cells (CD45$^-$CD235A$^-$) in CML and NBM. The horizontal bars represent median values and each dot represents data from an individual donor. The statistical differences were determined by unpaired Mann-Whitney test. (D-F) Impaired osteogenic and chondrogenic differentiation potential of CML-derived MSCs. (D) Representative images showing multilineage differentiation potential of NBM and CML MSCs. (E) Quantification of *in vitro* adipogenic and osteogenic differentiation of NBM and CML MSCs. Data were obtained from 2 independent experiments and each dot represents one replicate measurement. The statistical differences were determined by unpaired *t* test. Shown were results from one of 4 independent experiments. (F) GSEA plots showing the downregulation of osteoblast differentiation genes (right) and chondrocyte differentiation genes (left) in CML MSCs.
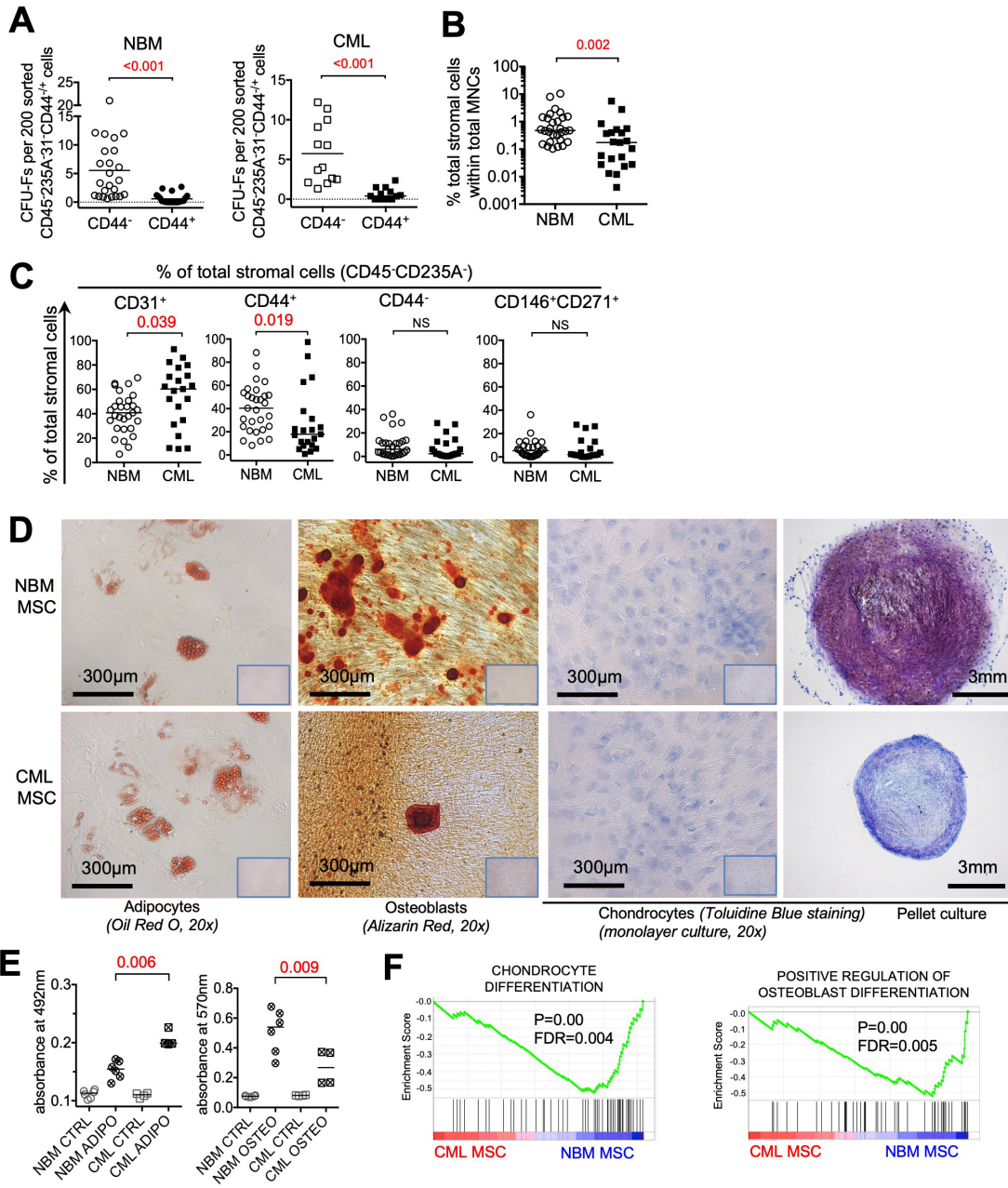
Related to Figure 1.

Figure S1

A
NBM — <0.001 — CFU-Fs per 200 sorted CD45⁻235A⁻31⁻CD44⁺/⁺ cells — CD44⁻ CD44⁺

CML — <0.001 — CFU-Fs per 200 sorted CD45⁻235A⁻31⁻CD44⁺/⁺ cells — CD44⁻ CD44⁺

B
0.002 — % total stromal cells within total MNCs — NBM CML

C
% of total stromal cells (CD45⁻CD235A⁻)

% of total stromal cells — CD31⁺ (0.039) — CD44⁺ (0.019) — CD44⁻ (NS) — CD146⁺CD271⁺ (NS) — NBM CML

D
NBM MSC / CML MSC

Adipocytes (*Oil Red O, 20x*) — 300µm

Osteoblasts (*Alizarin Red, 20x*) — 300µm

Chondrocytes (*Toluidine Blue staining*) (*monolayer culture, 20x*) — 300µm

Pellet culture — 3mm

E
0.006 — absorbance at 492nm — NBM CTRL, NBM ADIPO, CML CTRL, CML ADIPO

0.009 — absorbance at 570nm — NBM CTRL, NBM OSTEO, CML CTRL, CML OSTEO

F
CHONDROCYTE DIFFERENTIATION — Enrichment Score — P=0.00 FDR=0.004 — CML MSC / NBM MSC

POSITIVE REGULATION OF OSTEOBLAST DIFFERENTIATION — Enrichment Score — P=0.00 FDR=0.005 — CML MSC / NBM MSC

Figure 2. Absence of BCR-ABL fusion gene in CML stromal cells. Freshly sorted CD44⁻ MSCs, CD31⁺ ECs, CD44⁺ mature stromal cells and CD45⁺ hematopoietic cells from newly diagnosed CML patients and healthy controls were transferred to microscopic slides for FISH analysis. (A) The representative images of different BM stromal cell populations and hematopoietic cells after FISH analysis. (B-C) Summary table showing frequencies of *BCR-ABL1*⁺ cells in all BM stromal and hematopoietic cell populations from (B) CML patients (n=6) and (C) non-CML controls (n=3). From 10 to 100 cells in total in each sample were counted for calculating the frequency of *BCR-ABL1*⁺ cells.

Related to Figure 1.

Figure S2

A
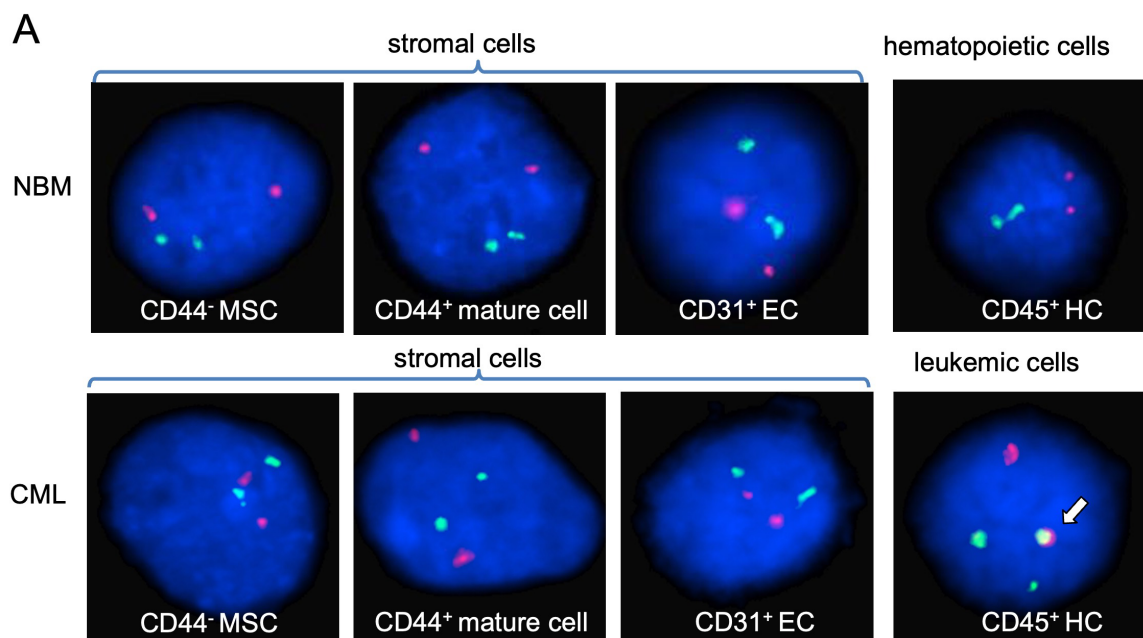
B

	CML10	CML11	CML16	CML20	CML22	CML25
CD44⁻ MSCs	neg	neg	neg	-	neg	neg
CD31⁺ ECs	-	-	neg	-	neg	neg
CD44⁺ mature cells	neg	neg	neg	neg	neg	neg
CD45⁺ HCs	100%	98%	95%	18%	88%	84%

C

	Ctrl1	Ctrl2	Ctrl3
CD44⁻ MSCs	neg	neg	neg
CD31⁺ ECs	-	neg	neg
CD44⁺ mature cells	-	neg	neg
CD45⁺ HCs	neg	neg	neg

Figure S3. RNA sequencing reveals molecular alterations of CML BM cellular niche components.

(A) Principal component analysis (PCA) plots showing distinct molecular profiles of the CD44$^-$ BM MSCs, CD31$^+$ ECs and CD44$^+$ mature stromal cells. (B) Volcano plot showing the altered genes in the CML CD44$^+$ mature stromal cells in comparison with their normal counterparts. (C-D) GSEA plots showing expression of selected genes sets related to cell cycle, MYC targets, and hematopoiesis maintenance in the CML MSCs and ECs. (E) Heatmap showing the top 50 up- and down-regulated genes in the CD44$^-$ CML MSCs and ECs. Red, highest expression; pink, moderate expression; light blue, low expression and dark blue, lowest expression. The arrows highlight the genes related to cell proliferation and inflammatory response.

Related to Figure 2.

Figure S3
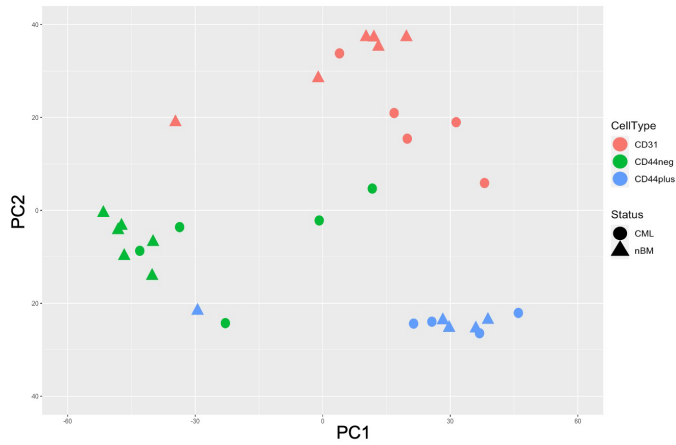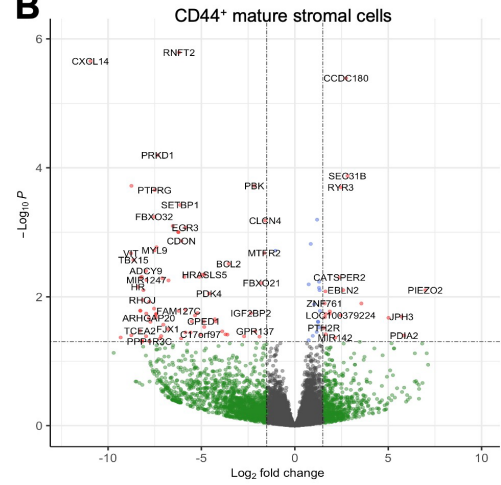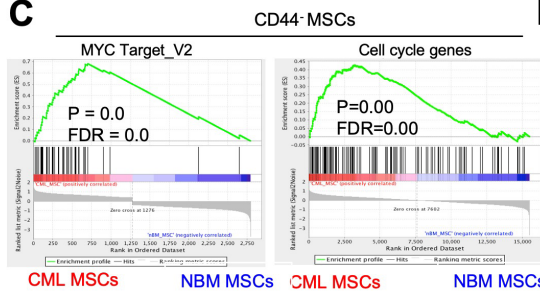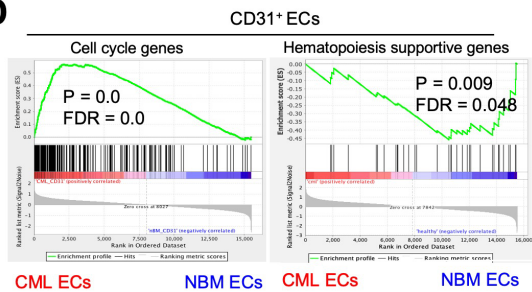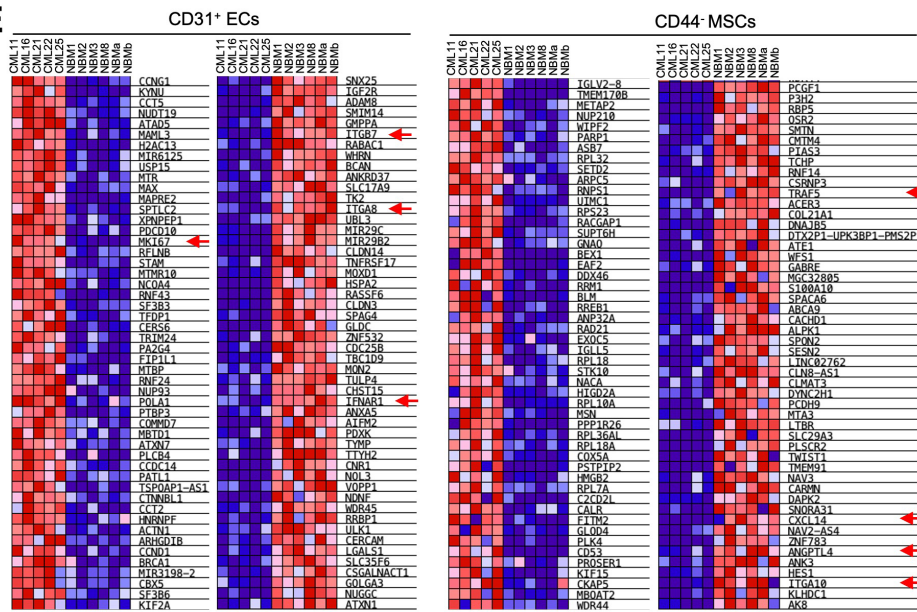
Figure S4. Q-PCR analysis confirmed downregulation of cytokines and growth factors in native CML MSCs and little or no expression of CXCL14 in hematopoietic cells.

(A) Relative expression of *CXCL12, ANGPT1, KITL, COL1A1, LAMA4, CXCL14* and *ANGPTL4* in freshly sorted MSCs from NBM (n=3-5) and CML patients (n=4). (B) Q-PCR analysis of *CXCL14* in the sorted T cells (CD3$^+$), monocytes (CD14$^+$), B cells (CD19$^+$) and HPCs (CD34$^+$CD38$^+$) from NBM (n=3) and CML patients (n=3) in comparison with that in NBM MSCs. (C-E) CXCL14 protein expression in the culture-expanded MSCs from healthy volunteers (NBM) and CML patients. (C) FACS dot plots showing expressions of CXCL14 in the NBM and CML MSCs at passage 2-3; (D) Histograms showing the intensity of CXCL14 in the NBM and CML MSCs; (E) Mean fluorescence intensity (MFI) of CXCL14 staining in the NBM and CML MSCs. The MFIs were normalized to that in the NBM MSCs included in each experiment. Each dot represents data from one patient. The numbers in the panel are *P* values determined by unpaired *t* test.
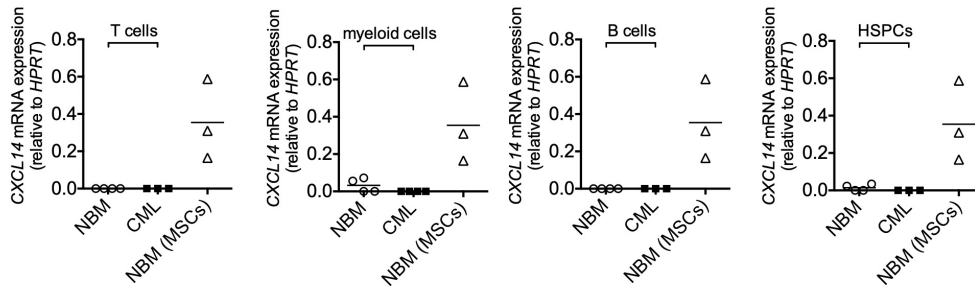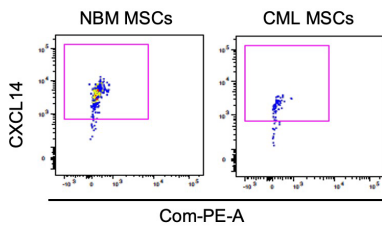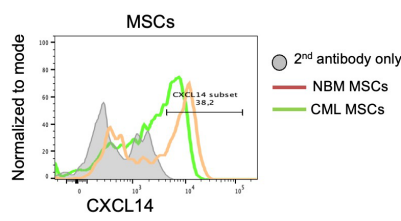
Related to Figure 2.

Figure S4

A
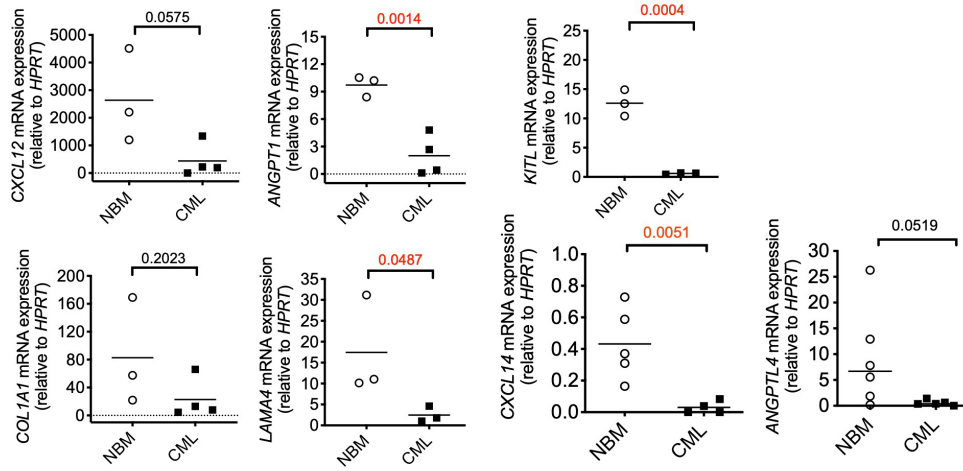
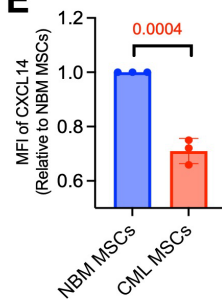
B

C

D

E

Figure S5. Altered expression of adhesion molecules in CML stromal cells.

(A) FACS analysis of adhesion molecules expression in MSC population (CD44⁻) in CML patients compared to age-matched healthy donors. (B) Representative histogram showing CD49D expression in NBM and CML MSCs. (C) FACS analysis of adhesion molecule expression in EC population (CD31⁺). Data are presented as % of the positive cells within total CD45⁻CD235A⁻CD31⁻CD44⁻ MSCs and CD45⁻CD235A⁻CD31⁺ ECs from CML patients and aged-matched NBM. Each dot represents the data from an individual patient.
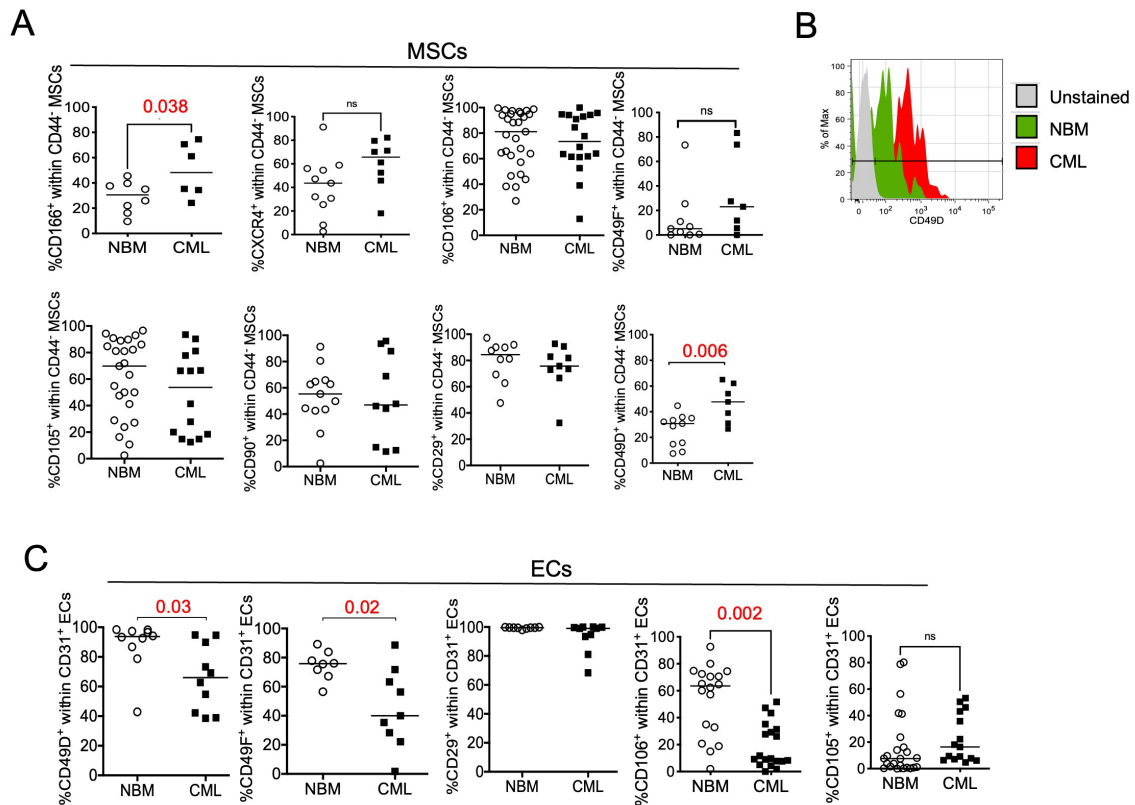
Related to Figure 2.

Figure S5

Figure S6. CXCL14 displayed little effect on healthy BM CD34$^+$CD38$^-$ stem and progenitor cells in co-cultures with primary CML MSCs.

(A) Experimental design for assessing the effect of CXCL14 on healthy BM CD34$^+$CD38$^-$ cells by cobblestone area-forming cell (CAFC) assays using primary CML BM MSCs. FACS-sorted BM MSCs from CML patients were expanded and plated one day prior to seeding normal BM CD34$^+$CD38$^-$ cells into the culture in presence of CXCL14 (10ng/mL) or PBS. The CAFCs were counted on day 14 and the colonies were subsequently transferred to methylcellulose for CFU-C assay. (B) CAFCs derived from healthy CD34$^+$CD38$^-$ cells co-cultured with CML MSCs. (C) CAFC-CFU-Cs derived from 100 healthy CD34$^+$CD38$^-$ cells initially co-cultured with CML MSCs for CAFC assay. Horizontal bars represent mean values, and each dot represents the average of triplicate measurements on an individual healthy donor. The statistical differences were determined by paired *t* test.
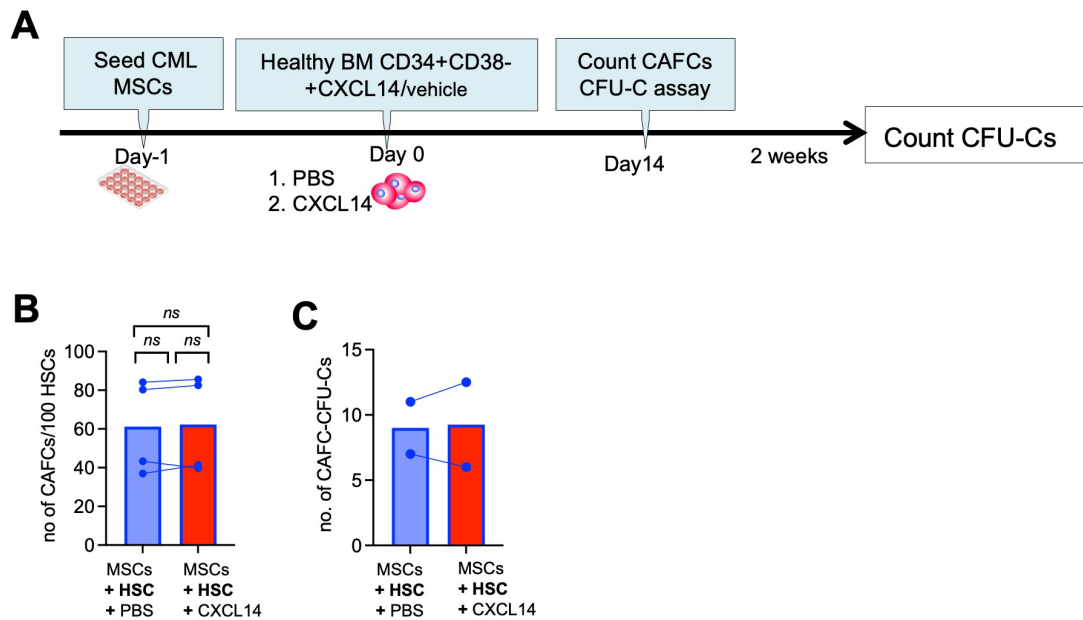
Related to Figure 4.

Figure S6

Figure S7. CML engraftment in the NSG-SGM3 mice prior and post CXCL14 and imatinib treatments. The blood was analyzed for human CD45$^+$ cells (patient CML cells) by FACS at 3 weeks post patient CML MNC injection. The mice with similar engraftment levels were distributed in each treatment group. (A) The % CML cells in blood of the NSG-SGM3 mice prior to the indicated treatment. Each dot represents single recipient mouse. Horizontal bars represent median values.(B) Representative FACS profiles showing gating strategy of hCD45$^+$ CML cells in the NSG-SGM3 recipient mouse BM, spleen and blood. The numbers in the panels are % of positive cells within total live (PI$^-$) cells. (C) The total BM cellularity and spleen size in the recipient mice at 1-day after 7-day treatment. Each dot represents single recipient mouse. (D) WBC, RBC and PLT counts in blood of the recipient mice at 1-day after 7-day treatment. (E) Total BM cellularity and spleen size in the recipient mice at 1-week after 12-day treatment. (F) WBC, RBC and PLT counts in blood of the recipient mice at 1-week after 12-day treatment.

 Related to Figure 5.

Figure S7

A

CML engraftment in blood 1 day before treatment
(3 weeks post transplantation)

B

Within PI- live cells

C

Post 7-day treatments

Total BM cellularity | Spleen size

D

Post 7-day treatments

WBCs | RBCs | PLTs

E

Post 12-day treatments

Total BM cellularity | Spleen size

F

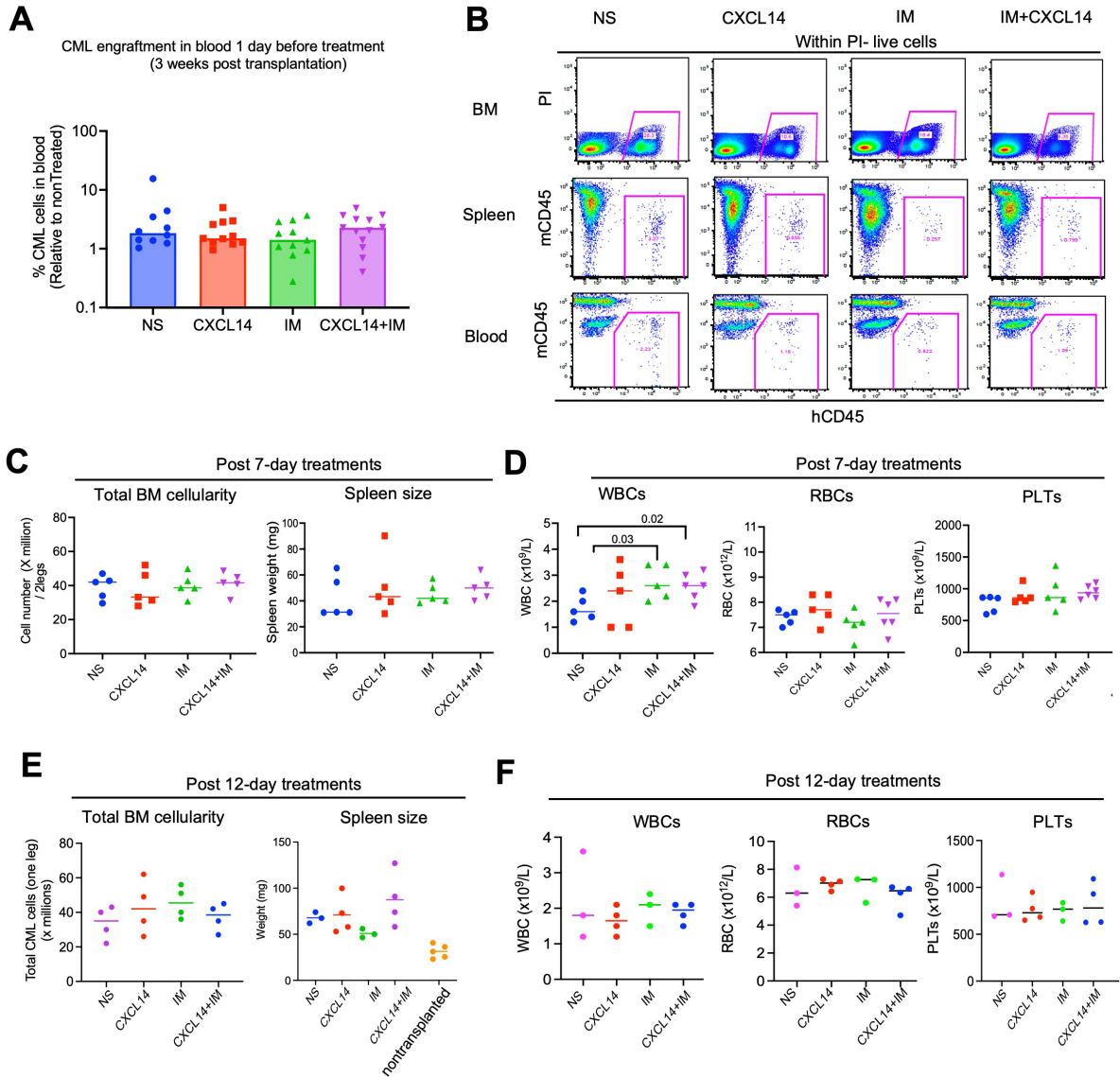Post 12-day treatments

WBCs | RBCs | PLTs

Figure S8. CML engraftment in primary and secondary recipient NSG-SGM3 mice following 10-12 day treatment with CXCL14 and/or imatinib.

(A) The % CML cells in the blood of the NSG-SGM3 mice 1 to 9 weeks post-treatment. Each dot represents single recipient mouse. The circle indicates a relapsed recipient mouse. (B) The % CML CD34$^+$ and CD34$^+$CD38$^-$ cells in BM of the NSG-SGM3 mice at 8 days after 12-day treatment. The transplanted CML cells were from a patient with a suboptimal TKI response. Each dot represents a single recipient mouse. The P value in the panel is determined by unpaired t test. (C) Representative FACS profiles showing the gating strategy of total hCD45$^+$ CML cells and CML CD34$^+$ cell subsets in the recipient BM. (D) The % of CML cells in the blood and BM of secondary recipients 3 and 6 weeks after secondary transplantation of one femur equivalent cells from the primary recipients mentioned in (B), respectively. The horizontal bars represent mean values.

Related to Figure 5.

Figure S8

A

1° recipients of CML55

relapsed

% CML cells in blood

- before treatment
- 1wk
- 3wks
- 5wks
- 9wks

DB: double treatment

NS   CXCL14   IM   CXCL14 + IM

B

1° recipients of CML62

X 2.5 fold

0.0165

% CD34⁺ CML cells of total live cells in BM

ns

% CD34⁺CD38⁻ cells of total live cells

NS   CXCL14   IM   CXCL14+IM

C

CML engraftment in BM in 1° recipients at 8 days post the last injection

PBS
CXCL14
IM
CXCL14+IM

hCD45 / mCD45
CD66B/CD15 / CD19
CD38 / CD34
CD38 / CD34

D

2° recipients of CML62

Blood, 3weeks

% CML cells in blood

BM, 5 weeks

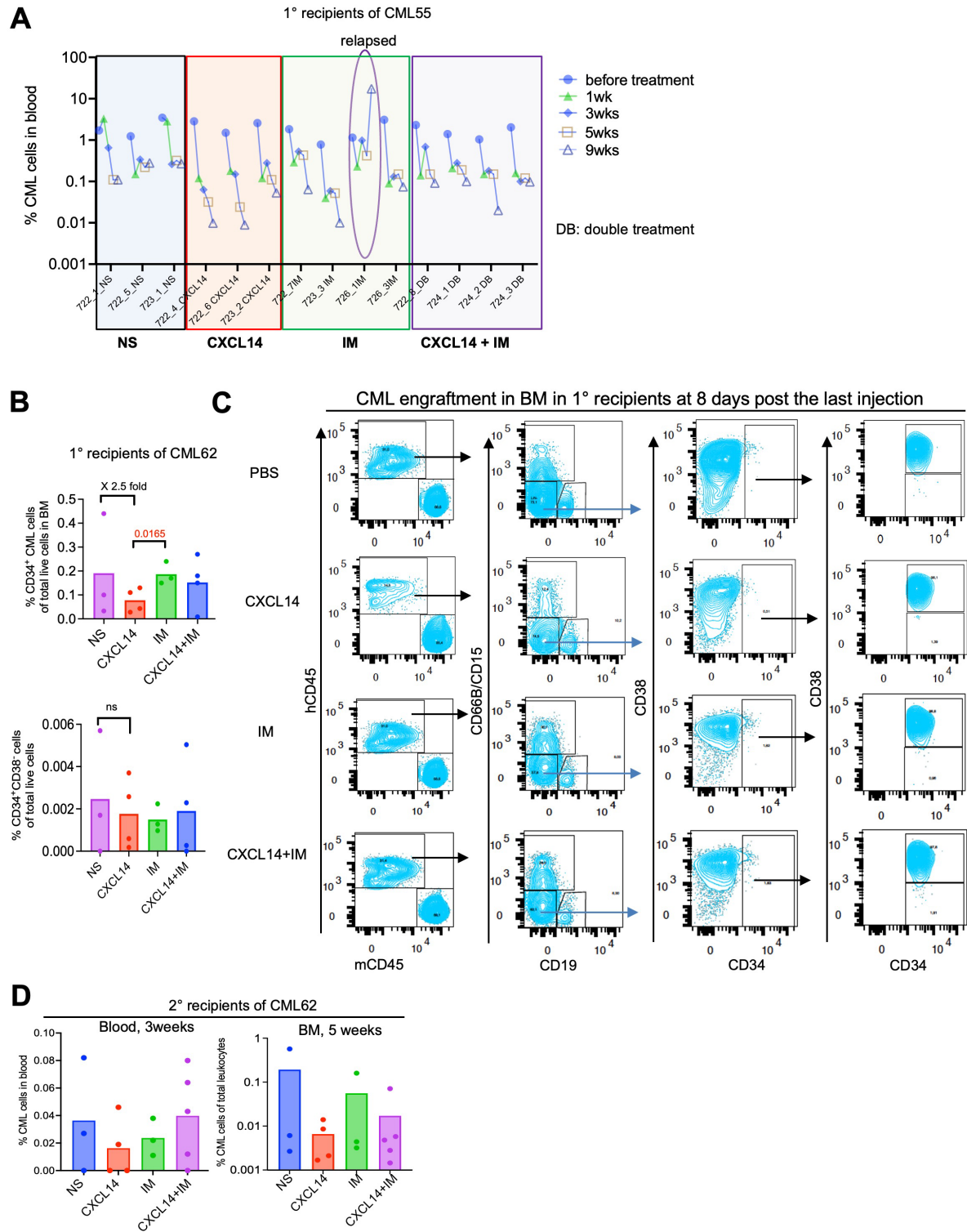% CML cells of total leukocytes

NS   CXCL14   IM   CXCL14+IM

Figure S9. Top 25 altered genes related to mTORC1 and OXPHOS and a hypothetical working mechanism of CXCL14 on CML LSCs.

(A) GSEA plot and heatmap showing the downregulated genes in mTORC1 signaling in the CXCL14-stimulated CML CD34$^+$CD38$^-$ cells. FDR, false discovery rate.

(B) GSEA plot and heatmap showing the downregulated genes in OXPHOS in the CXCL14-stimulated CML CD34$^+$CD38$^-$ cells.

(C) A hypothetical working model of CXCL14 is proposed based on the gene expression changes and the functional impact of CXCL14. After CXCL14 stimulation. The mTORC1 signaling in CML LSCs might be suppressed by CXCL14, which in turn could cause mTORC1 signaling suppression. This reduced signaling could subsequently downregulate MYC target genes and mitochondrial activities including OXPHOS and fatty acid metabolism, leading to reduced energy production and survival of CML LSCs. The dashed lines indicate the hypothetical molecular actions that need to be validated.

Related to Figure 6 and Figure 7.

Figure S9

Hypothetical working mechanism of CXCL14
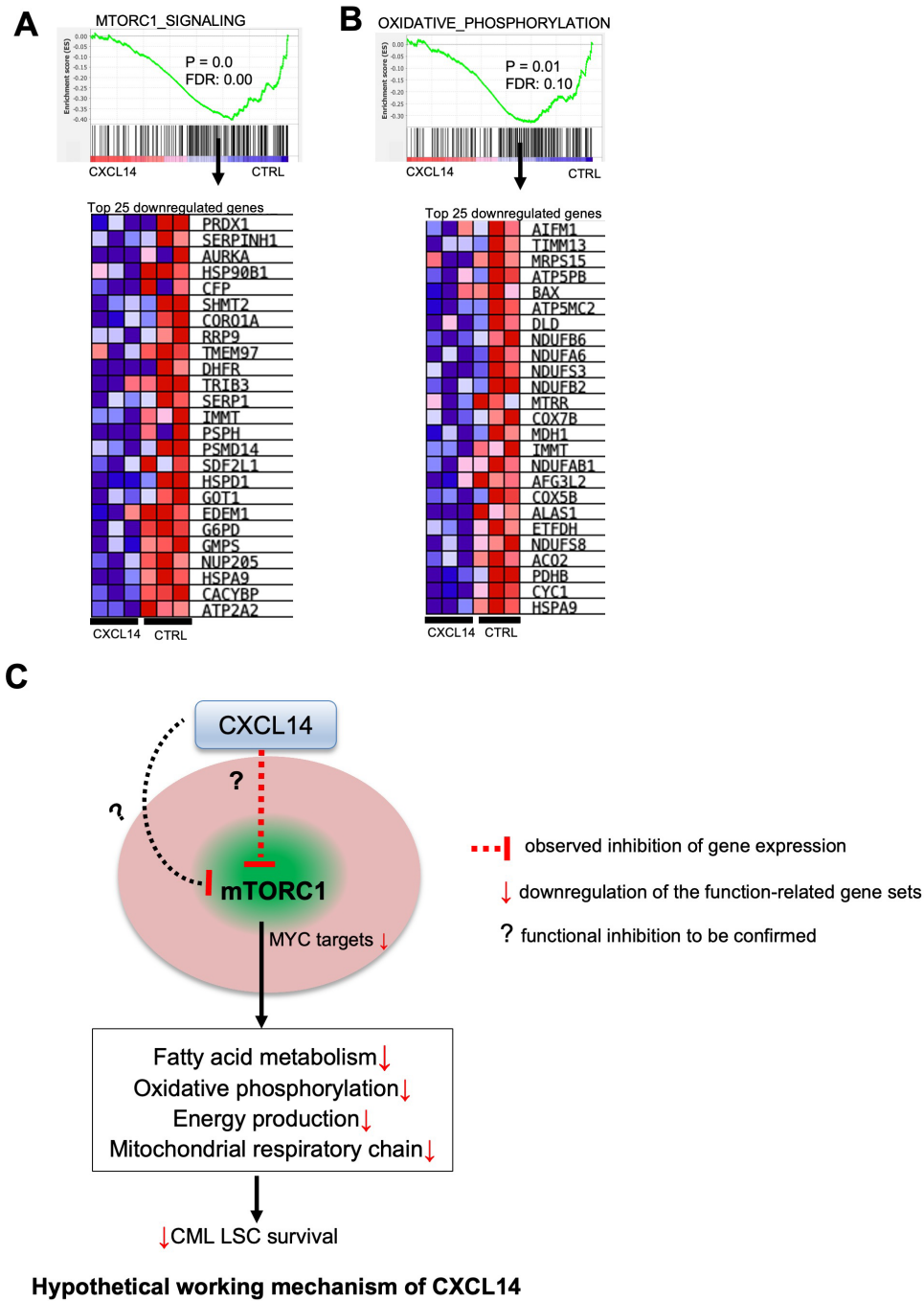
Supplemental references

1.   Qian H, Le Blanc K, Sigvardsson M. Primary mesenchymal stem and progenitor cells from bone marrow lack expression of CD44 protein. *The Journal of biological chemistry*. 2012;287(31):25795-25807.

2.   Dolinska M, Piccini A, Wong WM, et al. Leukotriene signaling via ALOX5 and cysteinyl leukotriene receptor 1 is dispensable for in vitro growth of CD34+CD38- stem and

progenitor cells in chronic myeloid leukemia. *Biochem Biophys Res Commun*. 2017;490(2):378-384.

3.   Kim D, Pertea G, Trapnell C, Pimentel H, Kelley R, Salzberg SL. TopHat2: accurate alignment of transcriptomes in the presence of insertions, deletions and gene fusions. *Genome Biol*. 2013;14(4):R36.

4.   Langmead B, Salzberg SL. Fast gapped-read alignment with Bowtie 2. *Nat Methods*. 2012;9(4):357-359.

5.   Li H, Handsaker B, Wysoker A, et al. The Sequence Alignment/Map format and SAMtools. *Bioinformatics*. 2009;25(16):2078-2079.

6.   Liao Y, Smyth GK, Shi W. featureCounts: an efficient general purpose program for assigning sequence reads to genomic features. *Bioinformatics*. 2014;30(7):923-930.

7.   Mortazavi A, Williams BA, McCue K, Schaeffer L, Wold B. Mapping and quantifying mammalian transcriptomes by RNA-Seq. *Nat Methods*. 2008;5(7):621-628.

8.   Robinson MD, Oshlack A. A scaling normalization method for differential expression analysis of RNA-seq data. *Genome Biol*. 2010;11(3):R25.

9.   Oliveros JC. An interactive tool for comparing lists with Venn's diagrams. http://bioinfogp.cnb.csic.es/tools/venny/index.html. *Venny*. 2007-2015.

10.   Wong WM, Dolinska M, Sigvardsson M, Ekblom M, Qian H. A novel Lin-CD34+CD38- integrin alpha2- bipotential megakaryocyte-erythrocyte progenitor population in the human bone marrow. *Leukemia*. 2016;30(6):1399-1402.

11.   Augsten M, Hagglof C, Olsson E, et al. CXCL14 is an autocrine growth factor for fibroblasts and acts as a multi-modal stimulator of prostate tumor growth. *Proc Natl Acad Sci U S A*. 2009;106(9):3414-3419.

12.   Cai H, Kondo M, Sandhow L, et al. Critical Role of Lama4 for Hematopoiesis Regeneration and Acute Myeloid Leukemia Progression. *Blood*. 2021.

13.   Xiao P, Sandhow L, Heshmati Y, et al. Distinct roles of mesenchymal stem and progenitor cells during the development of acute myeloid leukemia in mice. *Blood Adv*. 2018;2(12):1480-1494.

14.   Erny D, Dokalis N, Mezo C, Mossad O, Blank T, Prinz M. Flow-cytometry-based protocol to analyze respiratory chain function in mouse microglia. *STAR Protoc*. 2022;3(1):101186.